Waveguide Perturbation Techniques in Microwave Semiconductor Diagnostics*

K. S. CHAMPLIN†, MEMBER, IRE, AND D. B. ARMSTRONG†, STUDENT MEMBER, IRE

Summary—Scattering processes in semiconductors are often studied by observing scattering averages with measurements of various dc transport phenomena. With microwaves, the observation frequency can be of the order of the scattering frequency so that the corresponding microwave transport property may be complex. Thus, in studying detailed scattering mechanisms, a microwave transport experiment contains potentially more information than the analogous dc experiment. This paper discusses perturbation techniques which are useful in determining the microwave conductivity and low-field Hall effect of a bulk semiconductor contained in a waveguide from measurement of the properties of the transmitted wave.

I. Introduction

ELECTRICAL transport properties, such as conductivity and Hall effect, contain considerable information about the processes by which charge carriers in semiconductors are scattered[1] (*i.e.*, make spontaneous transitions between quantum states). Historically, dc measurements of transport properties have been a popular and useful tool of semiconductor research. The ac transport properties observed when the frequency of the electric field is comparable to the frequency of electron- or hole-scattering[2] differ from the dc properties by having frequency dependent real and imaginary parts. The added data conveyed in this case contain detailed information about the scattering mechanisms and energy band structure that is not found in the dc measurements.

This, then, is the primary advantage of measuring transport properties with microwaves rather than with dc. Microwave transport experiments are generally not well suited to exact analysis, however, because of the complex nature of the data, the relatively large losses in the material, and because normal modes are functions of the magnetic field. A further complication of microwave diagnostics (determination of material properties from microwave measurements) arises because transport properties are usually related to measured quantities by an inverse transcendental equation that cannot be expressed analytically.

* Received May 24, 1962; revised manuscript received October 10, 1962. This work was supported by the AF Office of Scientific Research of the Office of Aerospace Research under Contract No. AF 49(638)-747.

† Electrical Engineering Department, University of Minnesota, Minneapolis, Minn.

[1] See, *e.g.*, D. Long, "Scattering of conduction electrons by lattice vibrations in silicon," *Phys. Rev.*, vol. 120, pp. 2024–2032; December 15, 1960.

[2] The scattering frequency is defined to be $1/(2\pi\langle\tau\rangle)$ where $\langle\tau\rangle$ is the mean relaxation time of the carriers. For acoustical mode phonon scattering in either n-type silicon or p-type germanium, the scattering frequency is about 22 Gc at 77°K and decreases with decreasing temperature.

This paper provides the mathematical basis for determining the microwave conductivity and low-field Hall effect from measurements of the properties of a wave transmitted through a section of circular or square waveguide filled with the semiconductor and uniformly magnetized in the axial direction. The diagnostic procedure is taken in two steps:

1) Data obtained from measurements with a finite sample are converted to data for an infinite sample by numerically inverting a complex transcendental equation with a digital computer.
2) The microwave transport properties are then obtained with the aid of explicit expressions derived from perturbation theory.

The above two steps assume that the magnetic field causes only first-order changes in the spatial distribution and propagation constant, respectively, of the dominant TE waveguide mode. The diagnostic technique is therefore limited to low magnetic fields and does not apply to high-field behavior such as cyclotron resonance.

II. High-Frequency Transport Properties of Cubic Semiconductors

The relative permittivity of a cubic crystal that is uniformly magnetized in the Z direction is a tensor of the form

$$\overleftrightarrow{\epsilon_r} = \begin{Vmatrix} (\epsilon_r' - j\epsilon_r'') & -j(\eta' - j\eta'') & 0 \\ +j(\eta' - j\eta'') & (\epsilon_r' - j\epsilon_r'') & 0 \\ 0 & 0 & (\epsilon_r' - j\epsilon_r'') \end{Vmatrix} \quad (1)$$

to the first order in the magnetic field. Assuming spherical constant energy surfaces and no dispersion of the lattice relative permittivity ϵ_l, the tensor elements may be written

$$(\epsilon_r' - j\epsilon_r'') = \epsilon_l - j(\sigma_0/\omega\epsilon_0)\left[\left\langle \frac{\tau}{(1+j\omega\tau)} \right\rangle \Big/ \langle\tau\rangle\right] \quad (2)$$

and

$$(\eta' - j\eta'') = (\sigma_0/\omega\epsilon_0)\mu_{HO}B_Z\left[\left\langle \frac{\tau^2}{(1+j\omega\tau)^2} \right\rangle \Big/ \langle\tau^2\rangle\right] \quad (3)$$

where σ_0 and μ_{HO} are the dc conductivity and dc Hall mobility, respectively; B_Z is the magnetic flux density; and τ is the phenomenological relaxation time of the carriers.

The bracketed quantities[3] in (2) and (3) are, in general, complex and frequency dependent. Their real and imaginary parts are plotted in Figs. 1 and 2 for several types of scattering. One sees that the real and imaginary parts of both functions approach unity and zero, respectively, as $\omega\langle\tau\rangle$ approaches zero. For $\omega\langle\tau\rangle \ll 1$, the functions can be expanded to yield

$$\epsilon_r' = \epsilon_l - (\sigma_0/\epsilon_0)\frac{\langle\tau^2\rangle}{\langle\tau\rangle} \qquad \epsilon_r'' = (\sigma_0/\omega\epsilon_0)$$
$$\eta' = (\sigma_0/\omega\epsilon_0)\mu_{H0}B_Z \qquad \eta'' = 2(\sigma_0/\epsilon_0)\mu_{H0}B_Z\frac{\langle\tau^3\rangle}{\langle\tau^2\rangle}. \quad (4)$$

The general diagnostic problem will be to determine ϵ_r', ϵ_r'', η', and η'' for arbitrary $\omega\langle\tau\rangle$ from microwave measurements. The special case of $\omega\langle\tau\rangle \ll 1$, where (4) applies, is of special interest since it typifies room temperature conditions. A single transport experiment in this range, however, will convey only slightly more information than a dc experiment.

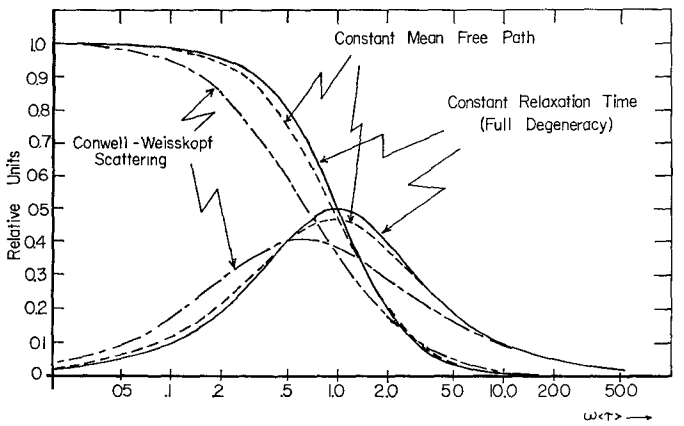

Fig. 1—Real and (negative) imaginary parts of bracketed conductivity term in (2). The real part approaches unity and the imaginary part approaches zero at low frequency.

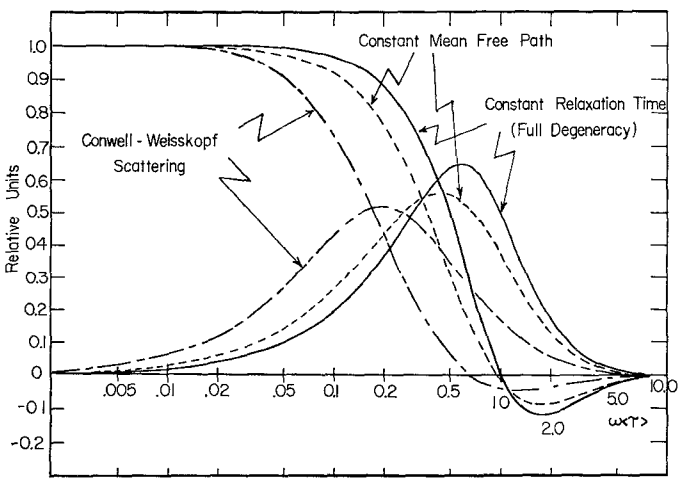

Fig. 2—Real and (negative) imaginary parts of bracketed Hall term in (3).

[3] The averages denoted by the symbol $\langle\ \rangle$ are Maxwellian averages weighted by the electron energy. For the mathematical definition, see, *e.g.*, R. A. Smith, "Semiconductors," Cambridge University Press, New York, N. Y., p. 111; 1959.

III. The Diagnostic Method

A. Correction for Finite Sample Length

Fig. 3 shows a section of circular or square waveguide filled with semiconductor between $Z=0$ and $Z=d$. In the empty part of the waveguide, both the clockwise (+) and counter-clockwise (−) circularly polarized dominant TE modes have identical propagation constant $\gamma_1^{\pm}=\gamma_1=j\beta_1$. Between $Z=0$ and $Z=d$, however, the degeneracy is removed by the axial magnetic field so that the corresponding propagation constants $\gamma_2^{\pm}=\alpha_2^{\pm}+j\beta_2^{\pm}$ differ from one another.

Because of the magnetic field, the field distributions of the normal modes in the filled section of waveguide are also different from those in the empty section. For arbitrarily large magnetization, this would result in a single incident mode exciting an infinite number of modes at $Z=0$ and $Z=d$. One can show, however, that for first-order changes in the field distributions, the change in the magnitude of the initially excited mode as well as the magnitude of the higher-order modes are at most of second order.[4] To the first order in the magnetic field, therefore, the transmission coefficients of the two circularly polarized dominant TE modes are still given by the well-known formula[5]

$$e^{-(A^{\pm}+j\Phi^{\pm})} = \frac{4\gamma_1^{\pm}\gamma_2^{\pm}}{(\gamma_1^{\pm}+\gamma_2^{\pm})^2 e^{\gamma_2^{\pm}d} - (\gamma_1^{\pm}-\gamma_2^{\pm})^2 e^{-\gamma_2^{\pm}d}} \quad (5)$$

just as without magnetic field.

Because of the disparity between propagation constants of clockwise and counter-clockwise dominant modes, a linearly polarized incident wave at $Z=0$ will emerge at $Z=d$ elliptically polarized with its polarization angle rotated. From the theory of the classical Faraday effect,[6] one can write

$$A = \frac{A^+ + A^-}{2} \qquad \Phi = \frac{\Phi^+ + \Phi^-}{2}$$
$$X = \frac{A^+ - A^-}{2} \qquad \Theta = -\frac{\Phi^+ - \Phi^-}{2} \quad (6)$$

where A is the change in the logarithmic amplitude and Φ is the change in phase of the transmitted wave, X is its ellipticity (ratio of minor to major axis), and Θ is its polarization angle. The quantities in (6) include the effects of multiple internal reflections. For an infinitely long sample, internal reflections are absent and the corresponding quantities are simply written

[4] H. Suhl and L. R. Walker, "Topics in guided wave propagation through gyromagnetic media, Part III—Perturbation theory and miscellaneous results," *Bell Sys. Tech. J.*, vol. 33, pp. 1160–1164; September, 1954.

[5] G. C. Montgomery, "Technique of Microwave Measurements," M.I.T. Rad. Lab. Ser., McGraw-Hill Book Co., Inc., New York, N. Y., vol. 11, p. 564; 1947.

[6] See, *e.g.*, K Försterling, "Lehrbuch der Optik," S. Hirzel, Leipzig, Germany, p. 44; 1928.

$$\alpha_2 = \frac{\alpha_2^+ + \alpha_2^-}{2} \qquad \beta_2 = \frac{\beta_2^+ + \beta_2^-}{2}$$

$$\xi_2 = \frac{\alpha_2^+ - \alpha_2^-}{2} \qquad \theta_2 = -\frac{\beta_2^+ - \beta_2^-}{2} \tag{7}$$

where α_2, β_2, ξ_2 and θ_2 are the change in logarithmic amplitude, phase, ellipticity, and polarization angle, respectively, of the elliptically polarized propagating wave (all per unit length).

Combining (5), (6) and (7) yields, to the first order in the magnetic field,

$$e^{-(A+j\Phi)} = \frac{4\gamma_1\gamma_2}{(\gamma_1+\gamma_2)^2 e^{\gamma_2 d} - (\gamma_1-\gamma_2)^2 e^{-\gamma_2 d}} \tag{8}$$

where

$$\gamma_1 = j\beta_1$$

$$\gamma_2 = \alpha_2 + j\beta_2$$

and

$$\xi_2 d = \frac{\partial \alpha_2 d}{\partial A} X - \frac{\partial \alpha_2 d}{\partial \Phi} \Theta$$

$$\theta_2 d = -\frac{\partial \beta_2 d}{\partial A} X + \frac{\partial \beta_2 d}{\partial \Phi} \Theta. \tag{9}$$

The first step of the diagnostic procedure may now be discussed with reference to Fig. 4. Interferometer measurements of A and Φ along with $\beta_1 d$ yield values of $\alpha_2 d$ and $\beta_2 d$ by a digital computer inversion of (8). Simultaneously, the computer uses (8) to calculate the four partial derivatives in (9). Finally $\xi_2 d$ and $\theta_2 d$ are determined from measurements of X and Θ with the aid of (9). We have programmed a computer to invert (8) by successive interpolation and to then evaluate the four partial derivatives numerically.

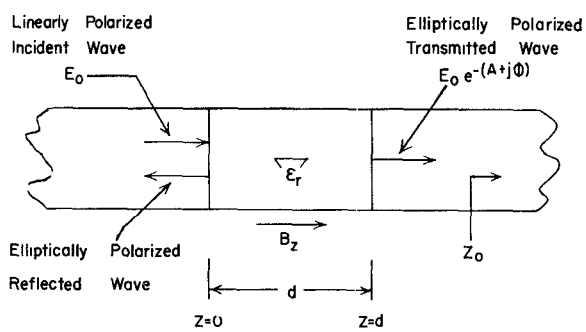

Fig. 3—Circular or square waveguide containing semiconductor. Linearly polarized TE wave is incident from the left.

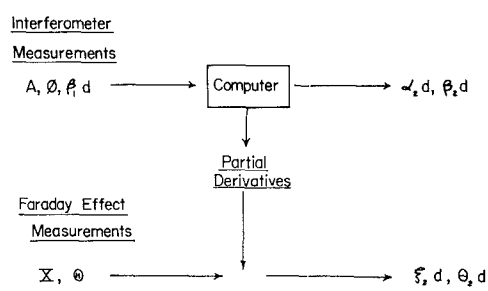

Fig. 4—First step of diagnostic procedure uses computer to invert complex transcendental equation and to calculate partial derivatives.

B. Explicit Expressions for Tensor Elements

The second step of the diagnostic procedure is made with the help of the well-known perturbation formula[7,8]

$$\gamma_2^{\pm} - \gamma_1^{\pm} = \frac{j\omega\epsilon_0 \int \{(\bar{\epsilon}_r - 1)\boldsymbol{E}_2^{\pm}\} \cdot \boldsymbol{E}_1^{\pm *} dS}{\int (\boldsymbol{E}_1^{\pm *} \times \boldsymbol{H}_2^{\pm}) \cdot \hat{k} dS + \int (\boldsymbol{E}_2^{\pm} \times \boldsymbol{H}_1^{\pm *}) \cdot \hat{k} dS} \tag{10}$$

Eq. (10) gives the difference between the propagation constants for a particular mode of the empty (subscript 1) and filled (subscript 2) waveguide sections, respectively, in terms of field distributions in those sections. The integrations are carried across the waveguide with $\hat{k}$ a unit vector in the axial direction.

Consider the two circularly polarized dominant TE modes of a circular or square waveguide. The fields in the empty section are of the form

$$\boldsymbol{E}_1^{\pm} = \boldsymbol{E}_1^x \pm j\boldsymbol{E}_1^y \qquad \boldsymbol{H}_1^{\pm} = \boldsymbol{H}_1^x \pm j\boldsymbol{H}_1^y \tag{11}$$

where the superscript indicates the polarization direction of the two degenerate linearly polarized modes which comprise the circularly polarized mode. To the zeroth order in the magnetic field, the electric field of the dominant modes in the filled section may be written

$$\boldsymbol{E}_2^{\pm} = \boldsymbol{E}_1^{\pm}. \tag{12a}$$

The corresponding magnetic field is then

$$\boldsymbol{H}_2^{\pm} = (\gamma_2^{\pm}/\gamma_1)\boldsymbol{H}_1^{\pm}. \tag{12b}$$

The first-order change in the propagation constant $\gamma_2^{\pm}$ follows by substituting (1), (11), (12a) and (12b) into (10). Noting that

$$\frac{\int \{\boldsymbol{E}_1^x \cdot \boldsymbol{E}_1^x\} dS}{\int \{(\boldsymbol{E}_1^x \times \boldsymbol{H}_1^y) \cdot \hat{k}\} dS} = \frac{j\omega\mu_0}{\gamma_1} \tag{13}$$

and defining the waveguide constant K as

$$K = \frac{\int \{(\boldsymbol{E}_1^x \times \boldsymbol{E}_1^y) \cdot \hat{k}\} dS}{\int \{\boldsymbol{E}_1^x \cdot \boldsymbol{E}_1^y\} dS} = \begin{cases} 8/\pi^2 \text{ for the square } TE_{10} \text{ mode} \\ 0.838 \text{ for the circular } TE_{11} \text{ mode} \end{cases} \tag{14}$$

[7] Suhl and Walker, *op. cit.*, pp. 1133–1194.

[8] K. S. Champlin and D. B. Armstrong, "Explicit forms for the conductivity and permittivity of bulk semiconductors in waveguides," PROC. IRE (*Correspondence*), vol. 50, p. 232; February, 1962.

yields

$$\{(\epsilon_r' - j\epsilon_r'') \mp K(\eta' - j\eta'') - 1\} = -\frac{(\gamma_2^{\pm} - \gamma_1)(\gamma_2^{\pm} + \gamma_1)}{\omega^2\mu_0\epsilon_0}. \quad (15)$$

Finally, explicit expressions for the four tensor elements are obtained by separating (15) into real and imaginary parts, then alternately adding and subtracting the four equations while applying (7) and ignoring second-order terms. The results, valid to the first order in the magnetic field, are

$$\{\epsilon_r' - 1\} = \left\{\frac{1}{\omega^2\mu_0\epsilon_0}\right\}\{\beta_2^2 - \alpha_2^2 - \beta_1^2\}$$

$$\epsilon_r'' = \left\{\frac{2}{\omega^2\mu_0\epsilon_0}\right\}\{\alpha_2\beta_2\}$$

$$\eta' = \left\{\frac{2}{\omega^2\mu_0\epsilon_0 K}\right\}\{\beta_2\theta_2 + \alpha_2\xi_2\}$$

$$\eta'' = \left\{\frac{2}{\omega^2\mu_0\epsilon_0 K}\right\}\{\alpha_2\theta_2 - \beta_2\xi_2\}. \quad (16)$$

Eq. (16) constitutes the second step of the diagnostic procedure. These equations apply for arbitrary $\omega\langle\tau\rangle$ as long as ξ_2 and θ_2 are proportional to B_Z. This restriction limits the magnetic field to the region

$$|\eta' - j\eta''| \ll |\epsilon_r' - j\epsilon_r''|. \quad (17)$$

The equations that apply with $\omega\langle\tau\rangle \ll 1$ are of interest. Combining (4) and (16) gives

$$\left\{\epsilon_l - \frac{\sigma_0}{\epsilon_0}\frac{\langle\tau^2\rangle}{\langle\tau\rangle} - 1\right\} = \left\{\frac{1}{\omega^2\mu_0\epsilon_0}\right\}\{\beta_2^2 - \alpha_2^2 - \beta_1^2\}$$

$$\sigma_0 = \left\{\frac{2}{\omega\mu_0}\right\}\{\beta_2\alpha_2\}$$

$$\sigma_0\mu_{H0}B_Z = \left\{\frac{2}{\omega\mu_0 K}\right\}\{\beta_2\theta_2 + \alpha_2\xi_2\}$$

$$\alpha_2\theta_2 \cong \beta_2\xi_2. \quad (18)$$

Because of the last relationship between the four variables, the dc Hall mobility can be written in either of two forms, each independent of frequency:

$$\mu_{H0} = \frac{1}{KB_Z}\left\{\frac{\beta_2}{\alpha_2} + \frac{\alpha_2}{\beta_2}\right\}\left\{\frac{\xi_2}{\alpha_2}\right\}$$

$$\mu_{H0} = \frac{1}{KB_Z}\left\{\frac{\beta_2}{\alpha_2} + \frac{\alpha_2}{\beta_2}\right\}\left\{\frac{\theta_2}{\beta_2}\right\} \quad (19)$$

for the special case of $\omega\langle\tau\rangle \ll 1$.

IV. Apparatus

Fig. 5 shows a typical germanium sample and circular sample holder for X-band measurement of conductivity and Hall effect. The accuracy of the measurements is somewhat dependent upon the quality of contact between sample and waveguide and can be improved by alloying an "ohmic" region around the sample periphery. The holder shown has been machined out slightly from one end to provide a small "ledge" for the sample to contact.

The interferometer used to measure A and Φ is a conventional waveguide bridge[9-13] as shown in Fig. 6. Troublesome internal reflections are minimized with the four tuners. Bridge balance is characterized by null output from the "magic" tee when the total attenuation and phase shift of the upper and lower arms are equal. Measurement is made by substituting a filled sample holder for an empty one while noting the change of the attenuator and precision short necessary to maintain balance. The change in attenuation and phase shift are equal to A and $(\Phi - \beta_1 d)$, respectively.

The polarization rotation angle Θ and ellipticity X are measured with the Faraday effect apparatus of Fig. 7.[14,15] With zero magnetic field, null output is obtained when the output waveguide is perpendicular to the input waveguide. Resistive films in the transitions minimize internal reflections under these conditions. The magnetic field rotates the plane of polarization and causes the output wave to be slightly elliptic. Adjustment of the rotating coupling for minimum output then yields Θ, while X is obtained by comparing the major and minor axes of the ellipse with the precision attenuator.

V. Conclusion

The preceding discussion has given the basis for a guided wave technique for measuring the complex microwave conductivity and Hall effect of semiconductors. Because of the complexity of the mathematics, a digital computer is employed in an intermediate step of the diagnostic procedure. The technique assumes only that the magnetic field is small and takes losses and internal multiple reflections into consideration exactly. Although the general analysis is independent of $\omega\langle\tau\rangle$, explicit expressions for Hall mobility are also derived which are valid for $\omega\langle\tau\rangle \ll 1$.

[9] T. S. Benedict and W. Shockley, "Microwave observation of the collision frequency of electrons in germanium," *Phys. Rev.*, vol. 89, p. 1152; March 1, 1953.
[10] T. S. Benedict, "Microwave observation of the collision frequency of holes in germanium," *Phys. Rev.*, vol. 91, p. 1565; September 15, 1953.
[11] J. M. Goldey and S. C. Brown, "Microwave determination of the average masses of electrons and holes in germanium," *Phys. Rev.*, vol. 98, pp. 1761–1763; June 15, 1955.
[12] F. A. D'Altroy and H. Y. Fan, "Effect of neutral impurity upon the microwave conductivity and dielectric constant of germanium at low temperatures," *Phys. Rev.*, vol. 103, pp. 1671–1674; September 15, 1956.
[13] D. B. Armstrong, "Waveguide Perturbation Technique for the Measurement of Microwave Conductivity and Permittivity of Thin Semiconductor Samples," M.S. thesis, University of Minnesota, Minneapolis; 1961.
[14] R. R. Rau and M. E. Caspari, "Faraday effect in germanium at room temperature," *Phys. Rev.*, vol. 100, pp. 632–639; October 15, 1955.
[15] J. K. Furdyna and S. Broersma, "Microwave Faraday effect in silicon and germanium," *Phys. Rev.*, vol. 120, pp. 1995–2003; December 15, 1960.

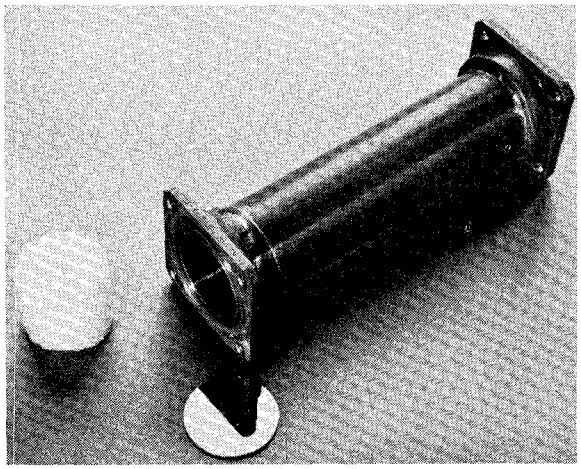

Fig. 5—Sample holder assembly for X-band measurements. Styrofoam plug holds semiconductor disc against "ledge" in waveguide.

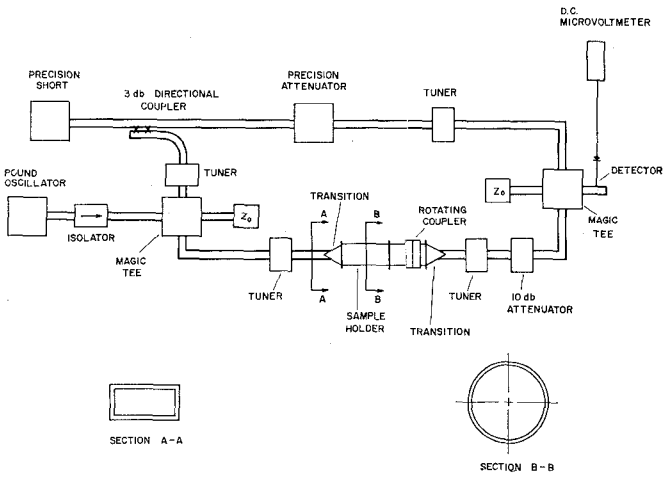

Fig. 6—Waveguide interferometer measures A and Φ.

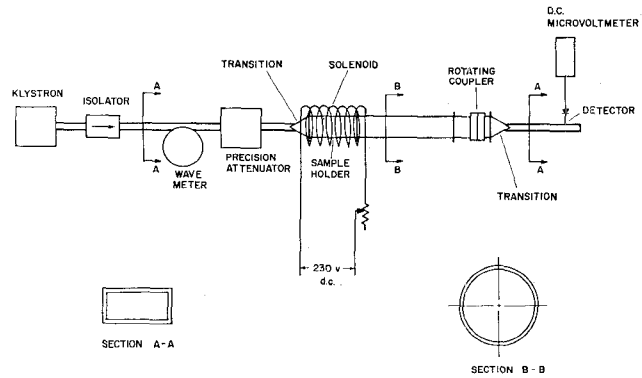

Fig. 7—Faraday effect apparatus measures X and Θ.